International Journal of Research Publication and Reviews

Journal homepage: www.ijrpr.com ISSN 2582-7421

Numerical Investigation on the Performance of Heat Transfer by Thermal Management System for Li-Ion Batteries using PCM

M.Sugumar[1], M. Shanmugam[1], Dr. S. Sundararaj[2], R. Loganathan[3], C. D. Meivelan[3], R. Mohan Raj[3], L. Muthukumar[3]

[1]Associate Professor, Department of Mechanical Engineering, Nandha Engineering college Erode, Tamilnadu-638052
[2]Professor, Department of Mechanical Engineering College,Sri Krishna College of Technology,Coimbatore,Tamilnadu-641008
[3]UG Students, Department of Mechanical Engineering, Erode, Tamilnadu-638052

ABSTRACT

This study investigates the usage of heat pipes (HP) and phase change materials (PCM) to regulate the temperature of lithium-ion power battery packs (LPBP). It is discovered that thermodynamic coupling has internal connected heat transport processes and a crucial application area for this discovery is offered. By applying the lumped parameter methodology and finite difference method, this mathematical model is created. If the theory of temperature control is demonstrated, then the internal heat flow distribution of a linked TM may be estimated to show that the theory holds true. Further parametric study of recent trend under various operating settings may therefore reveal the connected heat transfer mechanism and the needed application range. Single HP and PCM TM, on the other hand, result in higher battery surface temperature and a shorter control period when coupled with TM. The internal linked heat flux distribution transitions from Phase Change Material to Heat Pipe dominance, and this nearly entire relies on heat pipe in the end. Linked TM operates better under external circumstances of $0.2\ W/(mK) < k_{PCM} \leq 6\ W/(mK)$ and $h < 13\ W/m^2K$ in accordance with parametric investigation's findings.

Keywords: *Heat Pipe, Thermal Management, PCM, heat flux, Lithium-ion, Power Battery*

1. Introduction

Recently, the energy storing and power supply industries have been highly interested in commercial massive application of Lithium-ion Power Battery Packs (LPBP). For varying voltage and capacitance needs battery cells are stacked in both simultaneously and sequentially[1]. Heat dissipation is harmed as a result. This might cause permanent impacts such as capacity fading, internal breakdown, lifetime loss, and potentially significant safety concerns like as thermal runaway and explosion if the battery temperature is raised over the recommended operating temperature range (below 50ºC) [2]. In order to understand the thermal management of LPBP, it is necessary to do research.

Air/liquid TM requires an external circuit, which increases bulk cost, and complexity. Scholars are working to build TM that is not dependent on energy, such as HP and PCM, in order to make additional advancements[3]. Among the main reasons are HP's strong thermal conductivity and PCM's ability to maintain a consistent temperature on the surface.

As the working medium undergoes a phase shift, HP takes use of the working medium's high enthalpy in order to speed up heat removal. Li-ion battery cells/packs may be fast-charged using an HP thermal management system, according to [4]. After installing a heat pipe at a 60 W heat output rate, [5]found that the battery temperature dropped by 26.62 %. Using a single HP to cool a module resulted in a 42.1 % drop in module temperature compared to natural cooling, according to [6]. [7]studied the information on HP design. In terms of layout and liquid flow, vertical Plus horizontal pipes outperformed a single pipe[8].

In thermal management, Phase Change Material is commonly employed because of high enthalpy of phase transition and low temperature fluctuation. The temperature can also be more evenly distributed. PCM was originally used to battery thermal management by [9], who then used it to discharge a 100 Ah battery at conditions that were close to adiabatic. As a outcome of the PCM, the battery temperature was determined to be roughly 8°C lower than it would have been otherwise. Thermal conductivity has been a major issue with PCM [10]. As a result, LPBP TM was the attention of numerous writers due to its ability to improve heat transmission. [11], [12] researched together for additional fins to improve heat transmission area and shown that fins may significantly increase the amount of heat transferred and the temperature of a device. LPBP systems were compared to PCM and PCM expanded graphite [13]. Tests on battery surface temperature and uniformity of battery temperature indicated that PCM + expanded graphite was superior to conventional PCM graphite.

Single PCM thermal management does exist, however the condenser section's heat transfer intensity limits the thermal management of a single HP TM. In order to enhance temperature management, several researchers sought to combine PCM with HP[14]. Phase Change Material on the condenser of the

HP thermal management system enhanced battery pack temperatures and thermal balance, rendering to [15]. Using Phase Chang Material in an adiabatic portion of HP, [16] and [17] explored the improved effectiveness. In a study by [18], linked TM had a lower temperature peak when placed a top HP's evaporator portion. Another investigation found that the HP-liquid/PCM linked TM functioned well and was stable while cycling[19], [20].

HP/PCM linked TM investigations in the past published only the surface temperature history but did not show the idea of surface temperature history at all in the majority of studies. It is possible that the advantages of single and linked TM applications may change when functioning in different environments[21], [22]. HP/PCM coupled TM design requires immediate investigation of internal coupled heat transfer performance and application ranges.

Internally linked heat transfer mechanisms are revealed and a vital application range for coupled TM is proposed in this article. Finite difference and a consolidated parameter a variety of strategies are employed to achieve this goal. Internal heat flux distribution history of linked thermal management is examined in this research in addition to typical battery surface temperature analysis. The study above yields the most important assessment metrics[23]. If the trend of indicator variations under various operating conditions can be evaluated using parametric analysis, Heat transfer performance can be improved, and the crucial application range can be broadened[24].

2. Mathematical model

Lithium-ion power battery packs can be simplified by simulating one of the batteries. According to earlier research, the paper's HP/PCM linked TM can overcome the drawbacks of TM. When compared to other linked designs, it improves the battery's rate of heat release into the environment by increasing the heat transfer area or temperature differential. Although PCM is shown in Figure 1(b), it's clear that HP has a close relationship with the battery. HP's battery provides the initial source of heat for the evaporator. As evaporator temperatures rise, the driving force of temperature difference is altered. The PCM and surroundings are cooler in the condenser section than in the evaporator part. As a result, heat transfer 1 and 2 are both part of the process. In Figure. 1, single HP and Phase Change Material TM are displayed to establish the advantages of pair TM. Heat Pipe Thermal Management uses fins on the condenser part of the battery to improve the surface area and rate of heat convection. By transferring heat, one is able to reduce the amount of heat being rejected. On both sides of the cell, the PCM cools the battery and dissipates the heat-by-heat transfer TM. In this numerical analysis, half of the TM is chosen since its heat transport models are all symmetrical, as explained above.

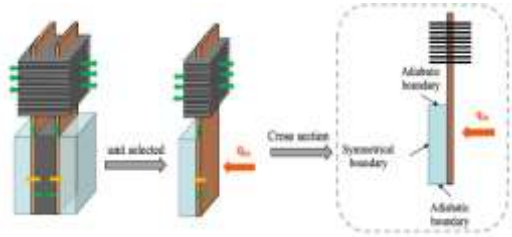

(a)

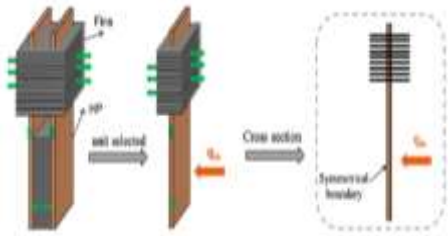

(b)

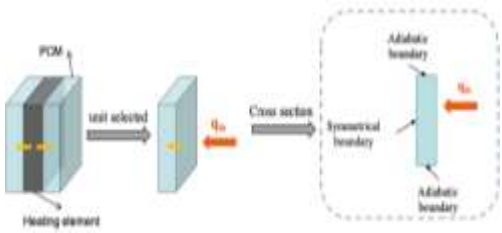

(c)

Fig. 1 Arrangement of Thermal Management (a) HP/PCM coupled (b)Heat Pipe (c) Phase Change Material.

Thermal management is the major focus of this study and the battery-operated is viewed as a source of heat, therefore a constant and steady source of power is selected. Due to the lack of heat convection in the grid, the further boundary conditions are set to adiabatic. Air heat conduction is insignificant to be taken into account. Distinct formulas are shown in 2-4, and the most important one is shown in equation (1)

$$cm\frac{\partial T}{\partial t} = k\frac{\partial^2 T}{\partial x^2} + S \quad (1)$$

2.1 Lumped-RC HP model

As soon as exposed to air, the working average converts to gas as a result of absorbing the heat from the battery. Heat convection is used to cool the heated vapor as it flows from the evaporator to the condenser and out into the environment. Working medium liquefies and returns to HP's bottom after releasing heat. It's continuing on like this for now.

The reduced value of the working medium, wall and wick's thermal resistances makes them insignificant.

- The working medium's thermal capacity is ignored;
- There are no considerations for liquid return or the enthalpy of vaporization.

There is a discrete equation constructed on the energy balance formula and Fourier Equation in Eq. (2), and the values necessary are presented in Table 1.

$$c_{HP}m_{HP}\frac{T_{sur}-T_{sur}^{0}}{dt} = q_{in} - \frac{T_{sur}-T_a}{R_{conv}} \quad (2)$$

Natural convection thermal resistance (R_{conv}) and Effectiveness HP heat capacity (C_{HP}) are stated in Equation. (3) -(5)

$$c_{HP}m_{HP} = c_{wall}\,m_{wall} + c_{wick}\,m_{wick} \quad (3)$$

$$R_{conv} = \frac{1}{h\cdot A_{root}+\xi\cdot h\cdot A_{fins}} \quad (4)$$

Using natural convection, the heat transfer coefficient is computed.

$$Nu = \frac{h\cdot H_C}{k_{air}} = \{0.59(Gr\cdot Pr)^{\frac{1}{4}}, Gr\cdot Pr < 10^9\ 0.1(Gr\cdot Pr)^{\frac{1}{3}}, Gr\cdot Pr \geq 10^9 \quad (5)$$

2.2.1*D − RC PCM model*

Despite the fact that standard PCM can absorb a considerable quantity of heat with little temperature increase, leakage is a restriction of thermal management applications. As a workaround this issue, [25] utilized a form-stable paraffin/expanded graphite compound Phase Change Material in their investigation. As may be seen in Table 1, the thermophysical characteristics are listed.

PCM is not suited for the lumped model because of the mobility of the phase change contact.

- Natural convection is not taken into account since paraffin/expanded graphite Phase Change Material is form-stable.
- Composite PCM's thermal-physical characteristics are assumed to remain constant.

A set of discrete formulas is provided in Eqs. (6a) to (6c) built on top of the Fourier law and the energy balance equation.

$$c_{PCM,i}m_{PCM,i}\frac{T_{PCM,i}-T_{PCM,i}^{0}}{dt} = q_{in} - \frac{T_{PCM,i}-T_{PCM,i,i+1}}{R_{PCM,i}/2}, i = 1 \quad (6a)$$

$$C_{PCM,i}m_{PCM,i}\frac{T_{PCM,i}-T_{PCM,i}^{0}}{dt} = \frac{T_{PCM,i-1,i}-T_{PCM,i}}{R_{PCM,i}/2} - \frac{T_{PCM,i}-T_{PCM,i,i+1}}{R_{PCM,i}/2}, i = 2,3\ldots n-1 \quad (6b)$$

$$C_{PCM,i}m_{PCM,i}\frac{T_{PCM,i}-T_{PCM,i}^{0}}{dt} = \frac{T_{PCM,i-1,i}-T_{PCM,i}}{R_{PCM,i}/2}, i = n \quad (6c)$$

$T_{PCM,ii+1}$ surface temperature among elements i and i+1, it may be computed as:

Table 1 Evaluation factors of HP and Phase Change Material.

HP		**PCM**	
(Cρ) wall ($J\cdot m^{-3}\ K^{-1}$)	4.43×10^6	k_{PCM} ($W\cdot m^{-1}\cdot K^{-1}$)	2.33
(Cρ) wick ($J\cdot m^{-3}\ K^{-1}$)	1.06×10^6	LH ($kj\cdot kg^{-1}$)	179
A_{root} (m^2)	0.0287	T_m (K)	316.16 – 318.16
A_{fins} (m^2)	0.0816	$(C\rho)_{pcm,s}/(C\rho)_{pcm,l}$ ($J\cdot m^{-3}\ K^{-1}$)	2.126×10^6
$H_{wall/wick}$ (m)	0.142	H_{PCM} (M)	0.142

$L_{wall/wick}$ (m)	0.12	L_{PCM} (M)	0.11

$$T_{PCM,i,i+1} = \frac{R_{PCM,i}}{R_{PCM,i}+R_{PCM,i+1}} \cdot T_{PCM,i} + \frac{R_{PCM,i+1}}{R_{PCM,i}+R_{PCM,i+1}} \cdot T_{PCM,i+1}, i = 1,2 \dots n-1 \quad (7)$$

If you know the temperature of a battery's surface, you can figure out its "surface temperature".

$$T_{sur} = T_{PCM,1} + \frac{1}{2} q_{in} \cdot R_{PCM,1} \quad (8)$$

Thermal Resistance and Active specific heat capacity are determined as Equation (9) and Equation (10) based on the phase transition process.

$$C_{PCM,i} = \{c_{PCM,s}, T_{PCM,i} \le T_m - \sigma \ \frac{C_{PCM,s}+c_{PCM,l}}{2} + \frac{LH}{2\sigma}, T_m - \sigma < T_{PCM,i} < T_m + \sigma \ C_{PCM,l}, T_{PCM,i} \ge T_m + \sigma \quad (9)$$

$$R_{PCM,i} = \frac{\delta}{H_{PCM} \cdot L_{PCM} \cdot k_{PCM}} \quad (10)$$

Analysis of heat transfer performance is aided by the use of PCI and LF. The LF displays the ratio of melted to total PCM at the phase transition interface, which is defined as the point of the first grid exceeding, T_m.

$$f_{PCM,i} = \{0, T_{PCM,i} \le T_m - \sigma \ \frac{T_{PCM,i}-T_m+\sigma}{2\sigma}, T_m - \sigma < T_{PCM,i} < T_m + \sigma \ 1, T_{PCM,i} \ge T_m + \sigma \quad (11)$$

$$LF = \frac{\sum_{i=1}^{n} f_{PCM,i}}{n} \quad (12)$$

2.3. HP/Phase Change Material joined model

Since the thermal resistances of the wall and wick are not taken into account, the surface temperature and HP temperature are the same. Because PCM absorbs heat from the HP evaporator, the PCM temperature at the PCM boundary is the same as the HP temperature. As an outcome, the temperature of the surface is the same as the HP's. As indicated in Fig. 2, Tsur. connects the HP and Phase Change Materials, respectively.

Expression for the results are shown in Equation (6c). According to Equations (13) and (14), there are differences in the expressions of the variables, T-sur and T-PCM.

$$T_{sur} = \frac{\frac{2}{R_{PCM,1}}}{\frac{2}{R_{PCM,1}} + \frac{c_{HP} \cdot m_{HP}}{dt} + \frac{1}{R_{conv}}} \cdot T_{PCM,1} + \frac{\frac{T_a}{R_{conv}} + \frac{c_{HP} \cdot m_{HP}}{dt} \cdot T_{sur}^0 + q_{in}}{\frac{2}{R_{PCM,1}} + \frac{c_{HP} \cdot m_{HP}}{dt} + \frac{1}{R_{conv}}} \quad (13)$$

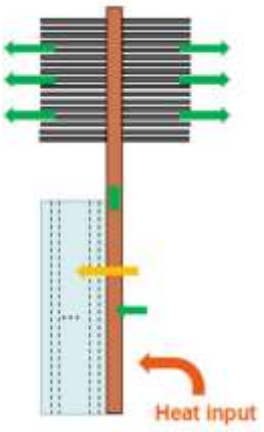

(a)

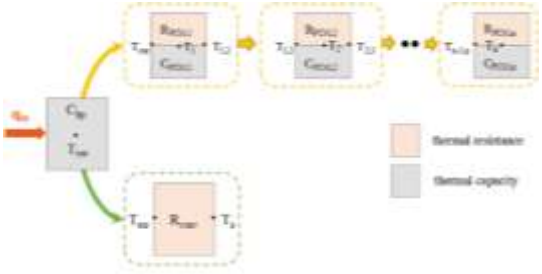

(b)

Fig. 2. Heat Pipe/Phase Change Material joined model (a) Structure (b) Networking.

$$c_{PCM,1} m_{PCM,1} \frac{T_{PCM,1}-T_{PCM,1}^0}{dt} = \frac{T_{sur}-T_{PCM,1}}{R_{PCM,1}/2} - \frac{T_{PCM,1}-T_{PCM,1,2}}{R_{PCM,1}/2} \quad (14)$$

QPCM/HP/total, PCM/HP are projected to analyze the thermal circulation of HP/Phase Change Material linked Thermal Management.

$$q_{total} = q_{HP} + q_{PCM} = \frac{T_{sur} - T_a}{R_{Conv}} + \frac{T_{sur} - T_{PCM,1}}{R_{PCM,1}/2} \quad (15a)$$

$$\varepsilon_{PCM} = \frac{\sum q_{PCM}}{\sum q_{total}} \quad (15b)$$

$$\varepsilon_{HP} = \frac{\sum q_{HP}}{\sum q_{total}} \quad (15c)$$

The tridiagonal matrix is obtained by sorting through the discrete equation, then the Thomas method is used to FORTRAN to finish the evaluation.

3. Results and discussion

3.1 Authentication of mathematical arrangement

The purpose of establish the models of mathematics correctness, two steps of validation are carried out. To begin, tests of independence are used to identify the proper grid size and time step. Findings may be compared to those of others after the grid and time stage are in place.

Verification

The Heat Pipe and Phase Change Material models are equated to earlier literature in order to authorize the correctness of the outcomes. According to the ASHRAE regulations, the values in Table 2 do not exceed 30 %.

$$NMBE = \sum_{k=1}^{m} \left| var_{present}(k) - var_{others}(k) \right| / \left(\underline{Var_{others}} \cdot m \right) \times 100\% \quad (16a)$$

$$RMSE = \sqrt{\frac{\sum_{k=1}^{m} \left(var_{present}(k) - var_{others}(k) \right)^2}{n}} / \underline{var_{others}} \times 100\% \quad (16b)$$

$$ME = m \left\{ \left(var_{present}(k) - var_{others}(k) \right) / \underline{var_{others}} \mid k = 1,2,\ldots m \right\} \quad (16c)$$

3.2 Heat flux distribution and impact of temperature control

According to Fig. 4, three distinct thermal managements are shown, and the comprehensive analysis follows: Condenser heat exchange is the primary source of heat dissipation in HP TM. h and temperature differential among Heat Pipe and atmosphere ($\Delta T_{HP,a}$) influence the cooling capability of the system, as shown in Equation (2). When h and, T-HP, a. is relatively modest at the start, heat loss (q_{out}.) is smaller than input of heat (q_{in}) therefore the temperature of surface remains to rise. H and $\Delta T_{HP,a}$. increase when temperatures rise, enhancing HP's capacity to perform. Finally, the surface temperature stays constant when q_{out} is equal to q-in. HP TM's startup time is so brief that it can be overlooked. As a result, the control temperature ($T_{control}$) seems to be the constant surface temperature and the control time (t_{end}) can run on forever. It seems HP TM can be utilized for surface temperature control over a long period of time, although the control may not be enough for the purpose.

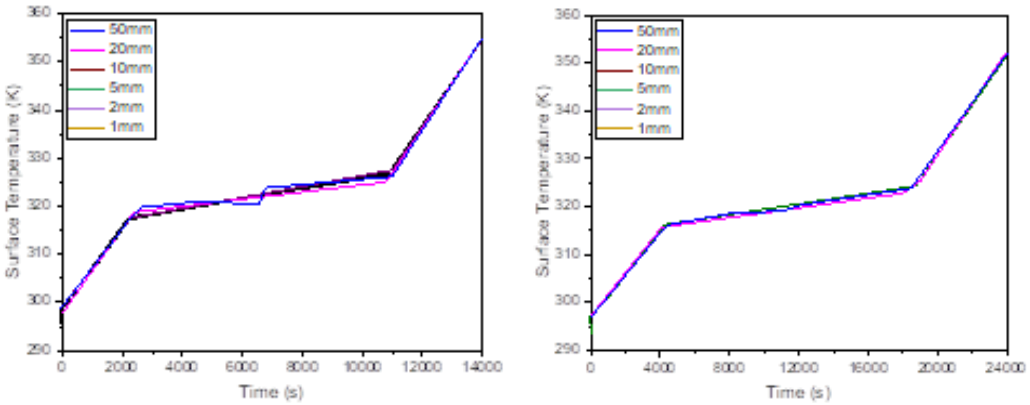

Fig. 3. Independent test on Grid (a) Phase Change Material (b) Heat Pipe/ PCM hybrid Thermal Management.

3.3 Phase Chase Material/Heat Pipe

In this construction, PCM absorbs all heat input. The sudden rise in temperature is owing to the Phase Change Material temperature being lower than T_m at the start. Afterwards, phase change takes over and the temperature is practically steady when it reaches [T_{m-s}, T_{ms}]. Overcoming T_{ms} virtually completely eliminates PCM's ability to influence surface temperature regulation. Due to this, $T_{control}$ can be modified by T_m, but the PCT may be too tiny to fulfill regular needs for $T_{control}$.

HP/PCM coupled TM

Heat absorption is shared across HP and PCM, which results in higher performance than using a single TM.

Table 2 Normalized Mean Biased Error, Root Mean squared Error and Maximum Error values for model Valuation.

	NMBENMBE	RMSE	MEME
PCM	3.19%	3.99%	7.72%
HP	0.35%	0.38%	0.54%

The terms, $T_{control}$ and t_{end} have the same meanings as PCM TM when considering the characteristics of surface temperature history curves. As can be shown in Figure 4, the linked TM $T_{control}$ temperatures stays at 316 K, which is 24 K less than the Heat Pipe Thermal Material temperature during the controller period. Additionally, t_{end} has a maximum extension duration of 1045 s, making it roughly 1.7 times longer than PCM TM. Fig. 5 examines the heat flux distribution history within the linked TM in great detail to better understand the concept of temperature history. You may find the driving force of distribution in Eq. (6a) by using the temperature differential between the surface and the initial variable temperature T_{sur}. As a result, the PCM state is used to divide the process into three steps.

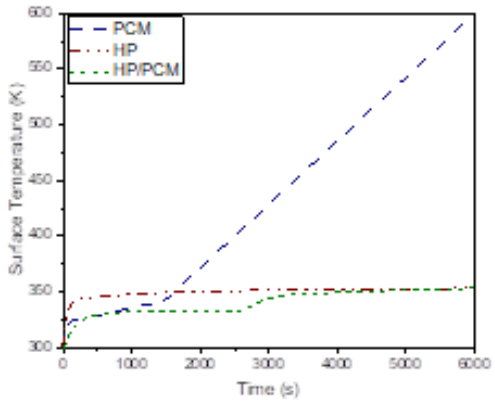

Fig. 4. Thermal Management of surface temperature data.

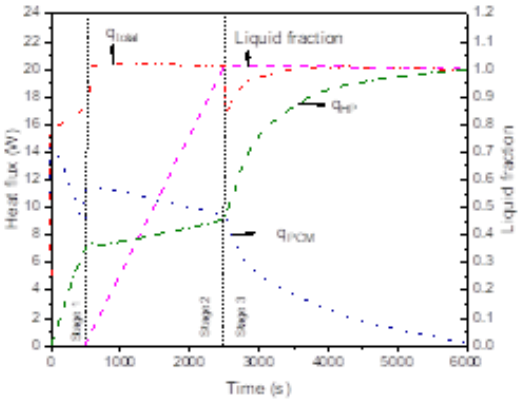

- **Stage 1:** A heat transfer mode without a switch in phase can only be used for the PCM portion, which has no liquid. When heat is transferred, T_{sur}, PCM. progressively diminishes, causing a rising-falling pattern in PCM's heat flux. Because q_{out}, q_{in} increases the heat flow of HP, T_{sur} and h continue to climb. PCM and, HP. are 76.1 % and 23.9 %, respectively, according to the formula. Consequently, PCM has a significant role to perform at this time.
- **Stage 2:** The liquid percentage increases from 0 to 1, indicating that melting has occurred. The enthalpy of phase transition and the progressive fall in, ΔT_{sur}, PCM1 respectively, cause a sharp rise in Q_{Pcm} and a subsequent dip in the graph. Q_{total} is infinitely near to qin, which causes a minor fluctuation in, T-sur and h, and therefore, q-HP. receives a tiny boost. This is seen in Figure 5. At this point, εPCM and ε HP account for 57.1 % and 42.9 % of total energy. PCM still plays a significant role in this time period, but its leadership position diminishes.
- **Stage 3:** A phase shift has occurred when the liquid fraction reaches 1 and the solid fraction reaches 0. q_{total} likewise decreases as a result of QPCM's decline, since perceptible thermal energy once again predominates. Batteries hold more energy, and thus, q-HP rises once again,

εPCM and ε HP. in this stage account for 9.4 % and 90.6 % of the heat input, respectively. It's clear that HP takes the lead role, and the PCM practically loses its ability to regulate temperature.

Coupled Thermal Management is primarily designed to decrease $T_{control}$ (related to Heat Pipe Thermal Management) and extend, t_{-end} (compared to HP TM) (comparative to HP TM). The inclusion of Heat Pipe lowers the amount of heat entering the PCM, hence extending the time it takes for the phase shift to occur. $T_{control}$. can be modified without being affected by external factors because to the PCM's integration. While PCM-dominant internal heat flow distributions are still present in HP/PCM linked thermodynamic models, the latter's near-total reliance on HP is evident.

3.4 Parametric study

External and artificial factors (h, W_{PCM}) are reviewed in this part, as well as six parameters of linked TM (T_a.) and 'k_{PCM}' that may affect the results. A critical application range for linked TM is proposed in this section, based on the external conditions and the factors effect on control on surface temperature and the dispersal of inner heat fluxes. In this range, artificial variables are the primary focus since developed to fit a certain set of circumstances. In spite of the fact that the data will vary, the same analytical procedure may be used for multiple purposes.

Impact of h and T_a

Enhancing HP's cooling capability by increasing h or by decreasing, T_a. reduces the strain on the PCM. Figures 6 and 7 depict the effects of h and, T_a. Here, the author uses h as a case study to demonstrate the similarities between two methodologies.

A Thermal Management connected in series is seen in Figure 7 (a) and (b) in terms of its surface and internal heat distribution. When h is increased, the ST decreases and PCM decreases as an entire. When h increases from 3 ($W/m^{-2}K$) to 9 (W/m^{-2} K), Phase Change Material is completely molten. From 10.52 to 6.06 kJ, Phase Change Material captures heat, while HP emits heat that increases from 11.41 to 17.35kJ in the same time period. Heat pipe regulated temperature is near or lower than Tm throughout stage 2, and PCM liquid % is approaching zero during this stage's average Phase Change Material fall from 15.84 (W/m^2K). Thermal management is HP's bread and butter. In addition, as shown in Fig. 7(b), εPCM decreases from stage 1 to stage 3 due to an increase in the amount of heat supplied to HP. In stage 1 and stage 2, the effects of ε PCM are clearly visible, but may be ignored when the temperature drops below h=13 (W/m^{-2}. K).

Comparing linked Thermal Management with single HP and Phase Change Material TM is the goal of Figure 7(c) and (d). In Figure. 7 (c), $\Delta T_{sur,HP,HP/PCM}$ (among the Heat Pipe and Thermal Management surface temperatures) shows a rising, steady and descending tendency over time. Although the effects of PCM are less noticeable, there are oscillations in the stored thermal energy at times like t=5000 and t=7000. Without phase change, Phase Change Material with lesser h has low influence, and it is tranquil in the PCM process for greater h at this duration, which causes temperature variation in the absence of heat transfer. Higher $\Delta T_{sur,\,HP,HP/PCM}$ can attain $90.98\,K$ at $1857\,s$ for $h = 3(\,W/m^2 \cdot K)$, and $\Delta T_{sur,HP,HP/PCM\ ap-}$ porches zero whereas $h \geq 13(\,W/m^2K)$. $\Delta t_{end,\,PCM,HP/PCM}$ in Fig. 7(d) becomes a rising tendency. This is because PCM TM and t_ are unaffected by changes in h that will be the end of it. The HP/PCM system "as h increases, so would the length of the arc. In adding, when $h \geq 13(\,W/m^2 \cdot K), \Delta t_{end,PCM,HP/PCM}$ inclinations to infinite. When paired TM, HP plays an important role because it's the most important portion, and $t_{end,HP/PCM}\ \ tends\ to\ infinite$.

Temperature control time can be extended and heat transport to PCM restricted by lowering the interior air temperature.

Effects of q_{in}

With an increase in qin, HP/PCM declines from 12.525 seconds to 10.10 seconds, as seen in Figure 8 (a) and (b).The average qp CM rises from 2.24 W to 29.32 W throughout level 2 of the experiment. As long as q_{in} is less than 5 W, HP is sufficient to dissipate the heat input and PCM is impervious to melting. As can be shown in Fig. 8 (b), PCM grows with increasing heat input in stages 1 and 2, but practically stays steady in stage 3. The following are the reasons behind this: When q_{in}. is increasing, qPCM-ascending PCM's rate outpaces, q_{HP} during stage 1. T_{sur} and, q_{HP} only vary in a short-range during stage 2, therefore more heat is sent to PCM for energy balance during this stage. Stage 3 saw the total melting of PCM, making the impacts of PCM in all of the situations seen in Fig. 8

Temperature rise is faster and more significant with a larger q_{in}. Fig. 8 shows how a coupled TM may regulate temperature down to T_m (c). Though, variation points appear at $q_{in} = 30\,W,\ 20\,W$ and $10\,W$ when $t = 3000\,s, 4000\,s$ and $7000\,s$, which signifies the end of the phase shift process. As defined earlier, Phase Change Material rises with q_{in} going mounting, so $\Delta t_{end,PCM,HP/PCM}\ \ reduces\ in$ Figure. $8(\,d)$. In additional, ε PCM is near to zero for $q_{in} \leq 5\,W$, thus $\Delta t_{end,PCM,HP/PCM}\ \ tends\ to\ infinity$.

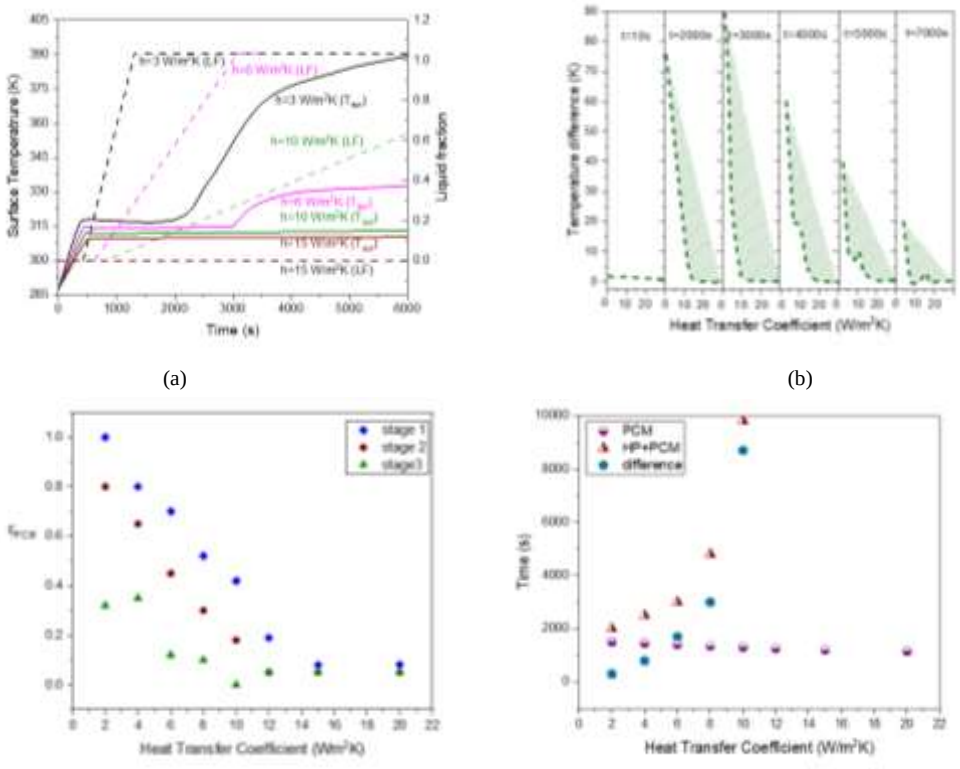

Fig. 6. Impacts of h (a) History of Surface temperatures (b) Phase Change Material proportion (c) Temperature Variation among Heat Pipe and coupled Thermal Management (d) Time control.

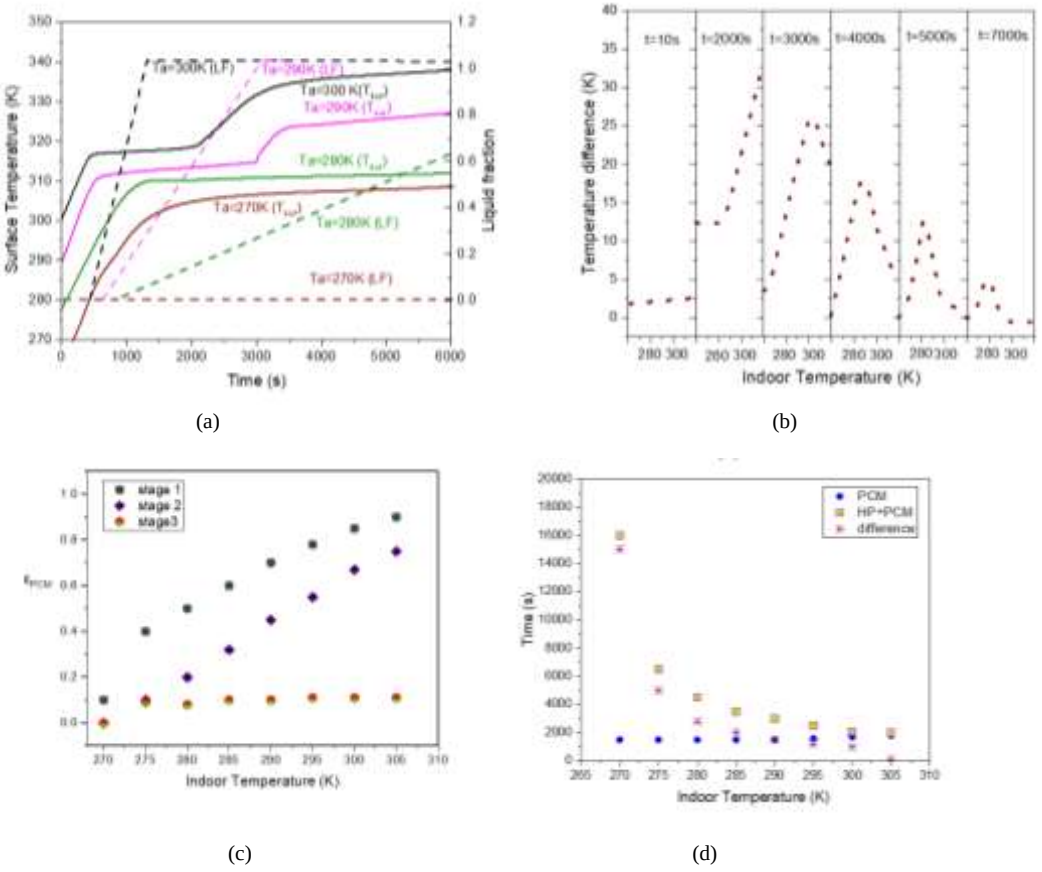

Fig.7. Impacts of Ta (a) History of Surface temperatures (b) Phase Change Material Proportion (c) Temperature variation among Heat Pipe and coupled Thermal Management (d) Time control

Effects of kPCM

$kPCM$ directly affects the PCM's heat transfer rate T_{sur} exceeds T_m because of the low heat transfer rate and hence more heat may escape from the Phase Change Material. Figs. 9(a) and 9(b) demonstrate the validity of this hypothesis through simulations. When k_{PCM} inexplicably $16\ W/(mK)$ to $0.2\ W/(mK)$, $T_{control}$ increases from $316.21\ K$ to $332.6\ K$, and εPCM through level 1 and level 2 also drops. Since the PCM absorbs less heat t_{end} extends for lower, $k_{PCM.}$ In Fig. 9(c), the time of $T_{sur,HP,HP/PCM}$ varies in three ways: up, up-down and down.

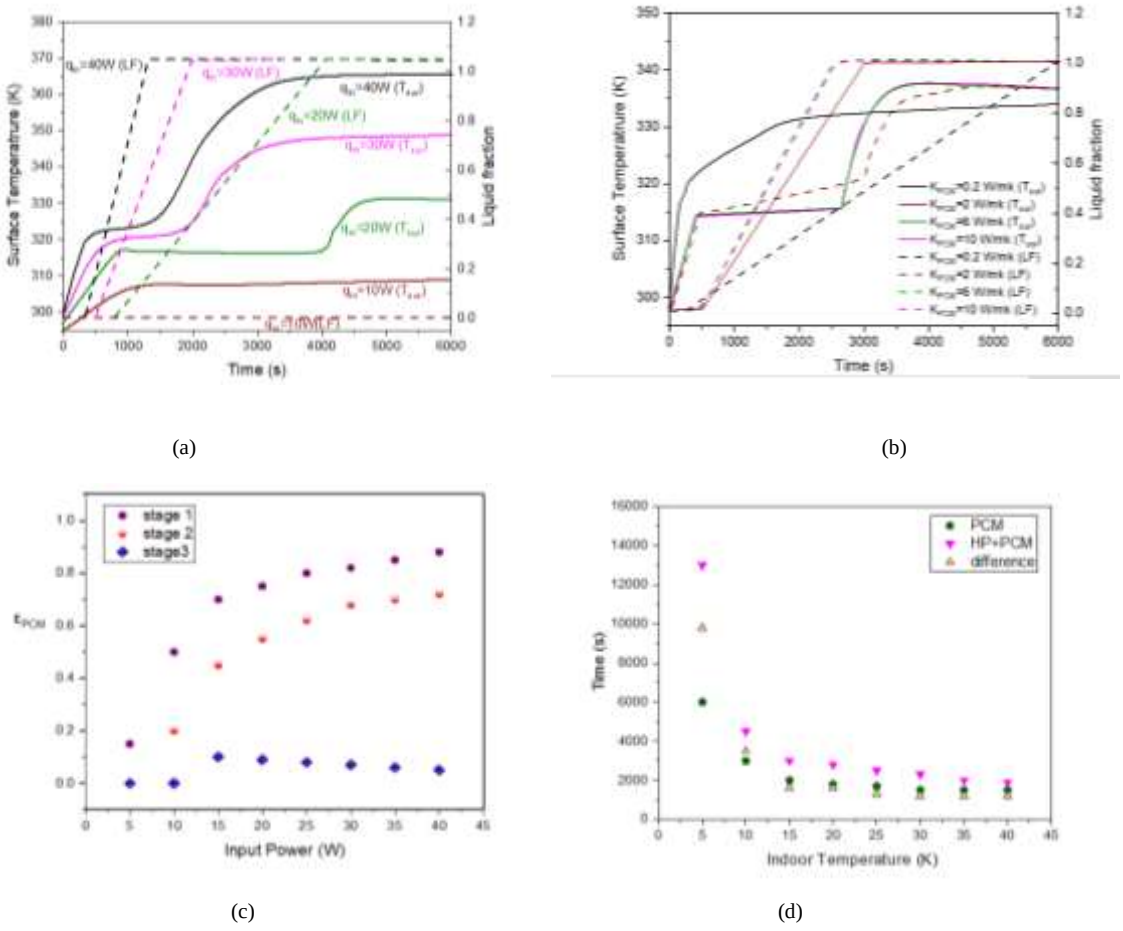

Fig. 8. Impacts of qin (a) History of Surface temperatures (b) Phase Change Material proportion (c) Temperature variation among Heat Pipe and coupled Thermal Management (d) Time control.

This is due to the fact that a lower k-PCM reduces the heat transfer rate of Phase Change Material in the early stages, but later on when PCM in other situations has already melted, it represents an advantage. Effects on linked TM are greater than those on PCM TM as seen in Figure. 9(d).

$\Delta t_{end,PCM,HP/PCM}$ *as well as rising . It is evident in Figure.* $9(b)$ *,* (d) *that PCM* is actually small for $kPCM^{PCM} = 0.2\ (W/mK)$ and almost ruins steady for $kPCM_{PCM} \geq 6\ (W/mK)$; hence $0.2\ (W/mK) < kPCM \leq 6(W/mK)$ is recommended for determining the rate of heat transfer and the enthalpy change in phase.

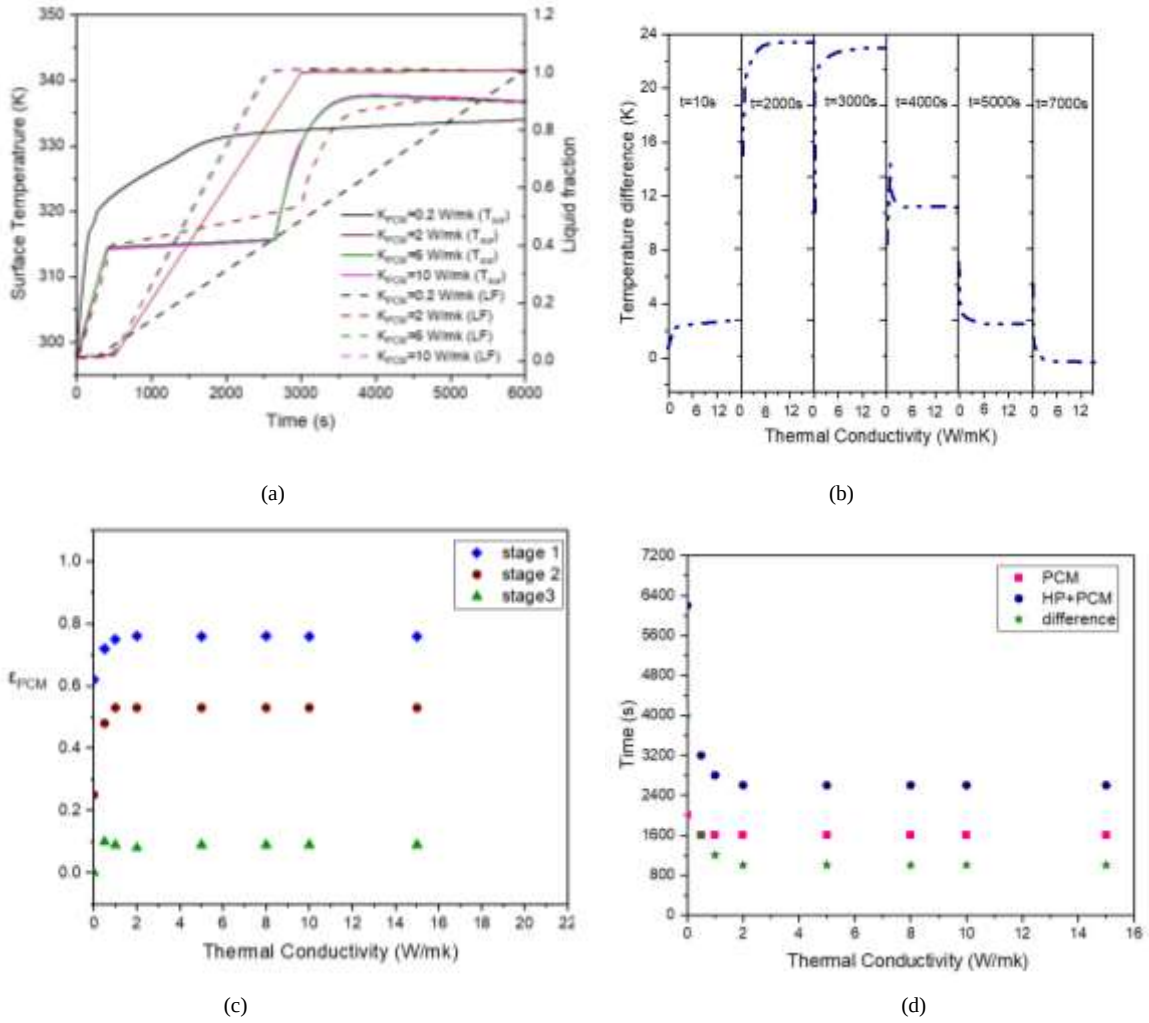

Fig. 9. Impact of kPCM (a) History of Surface Temperatures (b) Phase Change Material Proportion (c) Temperature variation among Heat Pipe and coupled Thermal Management (d) Time control.

Overall, the temperature control time may be extended and the surface temperature controlled more intensely by increasing the temperature control duration and decreasing the temperature control frequency (q_{in}, T_{a}.). In order to maintain a stable surface temperature, $T_{control}$ rises and the temperature control time increases, which is a two-pronged sword. There are several ways to limit the flow of heat from PCM to PCM via an internal linked heat transfer mechanism that are not dependent on W WCM's influence. When h is less than 13 (W/m^2K) and 0.2(W/m^2K) < K_{PCM}. < =6(W/m^2K) under the external conditions of this investigation, coupled TM is preferable. To choose WPCM, you need to consider your specific demands.

Conclusion

As a part of comparing the surface temperature history combined coupled and single TM, as well as the history of heat flux distribution in coupled TM, numerical models are established in this article. In an effort to better understand how these parameters change over time, more parametric study is conducted. The following are the findings' main conclusions:

The impacts of temperature management and the distribution of heat flux are examined using mathematical models. Coupled TM has a lower $T_{control}$ than the HP TM. It has been found that the end of connected TM is longer than the PCM TM, but it is still shorter than the PCM TM.

It's also worth noting that the internal heat flux distribution of connected Thermal Management transitions from Phase Change Material dominant to Heat Pipe dominant also eventually demonstrates practically total dependency on HP.

In-depth parametric research is conducted in a variety of working environments. The temperature control period may be extended by increasing the heat transfer coefficient, increasing the width of PCM and decreasing the heat input into the interior air. Thermal conductivity is diminishing as phase transition temperature rises, and the battery surface temperature rises as a result. Increasing the heat transfer coefficient, the temperature at which a phase shift takes place, and to decrease PCM's capacity to transfer internal energy, reduce input heat, temperature of air and thermal conduction in your home or workplace.

As indicated in the previous section, the crucial range of applicability is $h < 13\ W/m^2K$ and $0.2\ (W/m^2K) < kPCM_{PCM} \leq 6\ (W/m^2K)$ Throughout this study the environmental conditions to choose WPCM you need to consider your specific demands.

The crucial spectrum of application has improved thermal management effects when HP/PCM linked TM is taken into account holistically. However, because battery operation is long-term periodic, future study should look at the solidification process and changes in PCM's energy storage capacity. This paper, on the other hand, focuses solely on a single cooling approach for temperature management.

References

[1] C. Zhang, M. Yu, Y. Fan, X. Zhang, Y. Zhao, and L. Qiu, "Numerical study on heat transfer enhancement of PCM using three combined methods based on heat pipe," *Energy*, vol. 195, 2020, doi: 10.1016/j.energy.2019.116809.

[2] T.-H. Tran, S. Harmand, B. Desmet, and S. Filangi, "Experimental investigation on the feasibility of heat pipe cooling for HEV/EV lithium-ion battery," *Appl. Therm. Eng.*, vol. 63, no. 2, pp. 551–558, 2014, doi: 10.1016/j.applthermaleng.2013.11.048.

[3] J. Gou, W. Liu, and Y. Luo, "The thermal performance of a novel internal cooling method for the electric vehicle battery: An experimental study," *Appl. Therm. Eng.*, vol. 161, 2019, doi: 10.1016/j.applthermaleng.2019.114102.

[4] Y. Ye, L. H. Saw, Y. Shi, and A. A. O. Tay, "Numerical analyses on optimizing a heat pipe thermal management system for lithium-ion batteries during fast charging," *Appl. Therm. Eng.*, vol. 86, pp. 281–291, 2015, doi: 10.1016/j.applthermaleng.2015.04.066.

[5] N. Putra, A. F. Sandi, B. Ariantara, N. Abdullah, and T. M. Indra Mahlia, "Performance of beeswax phase change material (PCM) and heat pipe as passive battery cooling system for electric vehicles," *Case Stud. Therm. Eng.*, vol. 21, 2020, doi: 10.1016/j.csite.2020.100655.

[6] H. Behi *et al.*, "Thermal management analysis using heat pipe in the high current discharging of lithium-ion battery in electric vehicles," *J. Energy Storage*, vol. 32, 2020, doi: 10.1016/j.est.2020.101893.

[7] H. Behi *et al.*, "A new concept of thermal management system in Li-ion battery using air cooling and heat pipe for electric vehicles," *Appl. Therm. Eng.*, vol. 174, 2020, doi: 10.1016/j.applthermaleng.2020.115280.

[8] Q. Huang, X. Li, G. Zhang, J. Zhang, F. He, and Y. Li, "Experimental investigation of the thermal performance of heat pipe assisted phase change material for battery thermal management system," *Appl. Therm. Eng.*, vol. 141, pp. 1092–1100, 2018, doi: 10.1016/j.applthermaleng.2018.06.048.

[9] X. Jin *et al.*, "Structural design of a composite board/heat pipe based on the coupled electro-chemical-thermal model in battery thermal management system," *Energy*, vol. 216, 2021, doi: 10.1016/j.energy.2020.119234.

[10] R. J. Khan, M. Z. H. Bhuiyan, and D. H. Ahmed, "Investigation of heat transfer of a building wall in the presence of phase change material (PCM)," *Energy Built Environ.*, vol. 1, no. 2, pp. 199–206, 2020, doi: 10.1016/j.enbenv.2020.01.002.

[11] S. Al Hallaj and J. R. Selman, "Novel thermal management system for electric vehicle batteries using phase-change material," *J. Electrochem. Soc.*, vol. 147, no. 9, pp. 3231–3236, 2000, doi: 10.1149/1.1393888.

[12] S. Al-Hallaj and J. R. Selman, "Thermal modeling of secondary lithium batteries for electric vehicle/hybrid electric vehicle applications," *J. Power Sources*, vol. 110, no. 2, pp. 341–348, 2002, doi: 10.1016/S0378-7753(02)00196-9.

[13] H. M. Ali, "Recent advancements in PV cooling and efficiency enhancement integrating phase change materials based systems – A comprehensive review," *Sol. Energy*, vol. 197, pp. 163–198, 2020, doi: 10.1016/j.solener.2019.11.075.

[14] B. Zohuri, *Heat pipe design and technology: Modern applications for practical thermal management, second edition*. 2016.

[15] Z. Sun, R. Fan, F. Yan, T. Zhou, and N. Zheng, "Thermal management of the lithium-ion battery by the composite PCM-Fin structures," *Int. J. Heat Mass Transf.*, vol. 145, 2019, doi: 10.1016/j.ijheatmasstransfer.2019.118739.

[16] P. Ping, R. Peng, D. Kong, G. Chen, and J. Wen, "Investigation on thermal management performance of PCM-fin structure for Li-ion battery module in high-temperature environment," *Energy Convers. Manag.*, vol. 176, pp. 131–146, 2018, doi: 10.1016/j.enconman.2018.09.025.

[17] R. Huang, Z. Li, W. Hong, Q. Wu, and X. Yu, "Experimental and numerical study of PCM thermophysical parameters on lithium-ion battery thermal management," *Energy Reports*, vol. 6, pp. 8–19, 2020, doi: 10.1016/j.egyr.2019.09.060.

[18] W. Zhang, J. Qiu, X. Yin, and D. Wang, "A novel heat pipe assisted separation type battery thermal management system based on phase change material," *Appl. Therm. Eng.*, vol. 165, 2020, doi: 10.1016/j.applthermaleng.2019.114571.

[19] Z. J. Zuo and A. Faghri, "A network thermodynamic analysis of the heat pipe," *Int. J. Heat Mass Transf.*, vol. 41, no. 11, pp. 1473–1484, 1998, doi: 10.1016/S0017-9310(97)00220-2.

[20] K. Nithyanandam and R. Pitchumani, "Analysis and optimization of a latent thermal energy storage system with embedded heat pipes," *Int. J. Heat Mass Transf.*, vol. 54, no. 21–22, pp. 4596–4610, 2011, doi: 10.1016/j.ijheatmasstransfer.2011.06.018.

[21] Y. Cao and A. Faghri, "Transient two-dimensional compressible analysis for high-temperature heat pipes with pulsed heat input," *Numer. Heat Transf. Part A Appl.*, vol. 18, no. 4, pp. 483–502, 1991, doi: 10.1080/10407789008944804.

[22] W. Wu, W. Wu, and S. Wang, "Thermal optimization of composite PCM based large-format lithium-ion battery modules under extreme operating conditions," *Energy Convers. Manag.*, vol. 153, pp. 22–33, 2017, doi: 10.1016/j.enconman.2017.09.068.

[23] Z. Luo *et al.*, "Numerical and experimental study on temperature control of solar panels with form-stable paraffin/expanded graphite composite PCM," *Energy Convers. Manag.*, vol. 149, pp. 416–423, 2017, doi: 10.1016/j.enconman.2017.07.046.

[24] R. Huang, H. Wu, and P. Cheng, "A new lattice Boltzmann model for solid-liquid phase change," *Int. J. Heat Mass Transf.*, vol. 59, no. 1, pp. 295–301, 2013, doi: 10.1016/j.ijheatmasstransfer.2012.12.027.

[25] J. Qu, Z. Ke, A. Zuo, and Z. Rao, "Experimental investigation on thermal performance of phase change material coupled with three-dimensional oscillating heat pipe (PCM/3D-OHP) for thermal management application," *Int. J. Heat Mass Transf.*, vol. 129, pp. 773–782, 2019, doi: 10.1016/j.ijheatmasstransfer.2018.10.019